# Fracture behavior of filled elastomers: how do strain induced softening and its thermally induced recovery affect the fracture toughness?

I. Denora & C. Marano

*Dipartimento di Chimica, Materiali e Ingegneria Chimica "Giulio Natta", Politecnico di Milano, Piazza Leonardo da Vinci, 32, 20133 Milano, Italia*

ABSTRACT

In this work, two peroxide-crosslinked hydrogenated nitrile butadiene rubbers for hydrogen system applications have been studied. Both elastomers are carbon black filled and one of these also contains a small quantity of polyamide. At the beginning, a preliminary analysis of the strain rate effect on the mechanical response and of the strain-induced softening is reported. Moreover, the dissipated and stored energies involved in the deformation of both the virgin and softened materials are evaluated. The thermally induced recovery of the strain-softening is analyzed by performing two treatments. In the second part of the work, the fracture behaviour of the two materials is compared and the effects of softening and its thermally induced recovery on fracture behavior are evaluated on one of the two compounds. The main finding is that softened material has a lower fracture toughness compared to the virgin material, while toughness of the thermally treated softened material is comparable to that of the virgin one.

## 1 INTRODUCTION

Mechanical behaviour of carbon black reinforced elastomers is hysteretic and modifies when a deformation is applied. This consideration can be easily deduced from the analysis of the mechanical response of this type of materials when they are firstly subjected to a loading-unloading cycle and then to a second loading up to the same deformation level. First of all, during the first loading-unloading it can be observed that the material is not completely elastic, but it dissipates a quantity of energy that increases with the applied deformation. Moreover, it can be noticed that stress applied in the second loading is considerably lower than that of the first loading, while stress applied in the second unloading is comparable to that of the previous unloading. The softening induced by a deformation is generally referred to as *Mullins effect* (Mullins 1948, Mullins 1969, Diani et al. 2009). Major softening in the material is visible after the first applied strain while small differences are appreciable after the following ones.

It is still not clear what is the physical origin of this phenomenon: it could be traced back to ruptures of bonds between filler and polymer (Blanchard et al. 1952, Bueche 1960), molecules slipping over the surface of filler (Houwink 1956, Dannenberg et al. 1966, Rigbi 1968, Papkov et al. 1975), filler ruptures (Kraus et al. 1966) or disentanglements (Hanson et al. 2005). This change in the compound micro-structure is responsible of the lower dissipative behaviour of the previously stretched material compared to the virgin one, while the elastic response of these materials appears almost the same.

It has been observed by some authors that a recovery of the material structure modification due to deformation induced softening can be obtained by a proper thermal treatment or by solvent exposure (some examples in literature are Mullin 1948, Harwood and Payne 1966, Laraba-Abbes et al. 2002, Diani et al. 2009, Plagge and Kupple 2019 and Li et al. 2019).

Our research is part of a major project Polymers4Hydrogen which has the aim to develop new polymeric materials to be used in the hydrogen infrastructure. In this work, two carbon black filled hydrogenated nitrile butadiene rubbers have been investigated: one is a conventional grade while the other one was blended with polyamide, enhancing the thermal resistance of rubber (Hemstede-van Urk M. et al. 2020 and Handbook of Synthetic Rubber, Arlanxeo, 2021). This type of rubber is a promising one to be used in the energetic field and the full understanding of the applied deformation effect on its mechanical behaviour is important for the design of proper components for hydrogen system.

A preliminary characterization of the two materials was carried out to evaluate the effect of their different composition on their mechanical response.

Monotonic tensile tests in uniaxial loading conditions tests were initially performed at different strain rates. Loading-unloading tests were then carried out to compare the two materials with regard to both their dissipative behavior and their strain induced softening (Mullins effect). A study on the effect of a thermal treatment on the tensile behavior of the softened material was conducted for different thermal histories applied.

The materials fracture behaviour has been characterised through mechanical tests performed in quasi-static loading conditions on notched pure shear specimens and single edge notched tension (SENT) pieces. Energy-based fracture mechanics parameters have been used to assess fracture toughness at crack onset. Tests were performed on both virgin materials and softened ones before and after a thermal treatment defined on the basis of the preliminary characterization of the materials.

## 2 MATERIALS AND METHODS

### 2.1 *Materials and methods*

In this study, two filled elastomers provided by Arlanxeo have been investigated. They are two fully hydrogenated nitrile butadiene rubbers with 21% of acrylonitrile content. The amount of filler is the same in both compounds: in the first one (HNBR) there is carbon black while in the second one (HNBR-PA) carbon black and a small quantity of a thermoplastic polyamide (PA). The hardness is similar (79 and 82 ShA respectively).
Vulcanization was peroxide-based and was obtained by the compression moulding of the compounds at 170°C at a pressure of 10 MPa for 20 minutes. A post curing treatment has been applied at 160°C for 4 hours in order to complete curing process. Dumbbell specimens with a gauge length of 25 mm and tensile test pieces for SENT specimens have been die-cut from about 2 mm thick sheets obtained by a rectangular mould. Pure shear specimens have been produced with home-made moulds. Single edge notches were introduced with a blade at mid height in both pure shear and SENT specimens. In Table 1 information about specimens for fracture tests specimens are shown.

All the mechanical tests were carried out on an Instron 5967 dynamometer at 23°C in a displacement control mode at the displacement rate of 7.5, 10, 75 and 750 mm/min. Tests were video-recorded in order to measure deformations by Digital Image Correlation analysis (subset size=33 pixels and step size= 3 pixels).

Table 1. Fracture tests specimens features

| **Specimen** | **Features** |
|---|---|
| Notched SENT | Notched tight strips (width=15mm, gauge length=100mm, nominal notch length=6mm) as suggested in Agnelli et al. 2020 |
| Notched pure shear | Notched wide strips (width=98mm, gauge length=19.6mm, nominal notch length=15mm) (Yeoh, 2001) |

## 3 RESULTS

### 3.1 *Monotonic tensile tests*

As a preliminary characterization of the two compounds, their mechanical response dependence on the strain rate have been evaluated. In Figure 1 results of uniaxial tensile tests on dumbbell specimens are reported: it can be observed that for both the materials there is no difference in the mechanical response in tests performed at 7.5 and 75 mm/min, while they both appear stiffer at 750 mm/min. Mechanical behaviour of the two materials has been compared in Figure 2. As expected, the two elastomers show a similar behaviour, but HNBR-PA is stiffer.

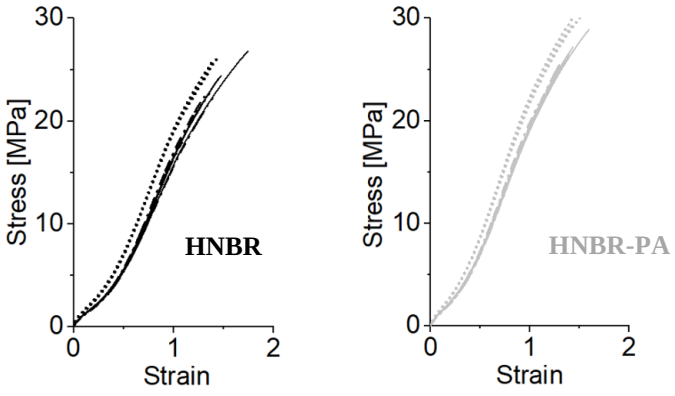


Figure 1. Stress-strain curves of the two materials at different strain rates.

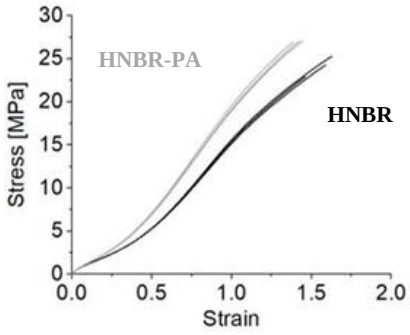


Figure 2. Comparison of stress-strain curves of the two materials.

### 3.2 *Loading unloading tests*

#### 3.2.1 *Single cycle tests*

Uniaxial tensile cyclic tests have been performed at the displacement rate of 75 mm/min in order to evaluate the strain energy components for the two materials. Several specimens have been loaded up to a certain value of maximum displacement and then unloaded to zero force. Three specimens have been tested for each maximum displacement applied, to evaluate the repeatability of results. In Figure 3 stress-strain curves of single cycle loading-unloading tests are reported for the two materials. The deformation strain energy density ($u_t$) has been calculated as the integral of the stress-strain loading curve. Its two components (stored, $u_s$, and dissipated energy densities, $u_d$) have been measured, respectively as the integral of the stress-strain unloading curve and the difference between $u_t$ and $u_s$ (Figure 4).

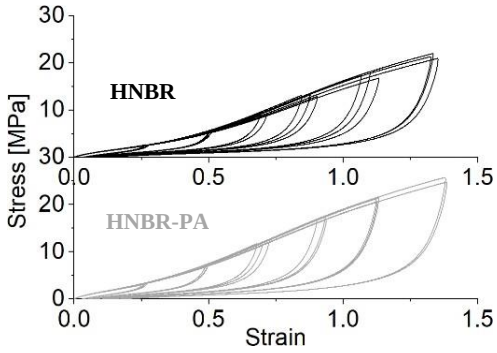


Figure 3. Single cycle loading-unloading tests for the two studied materials.

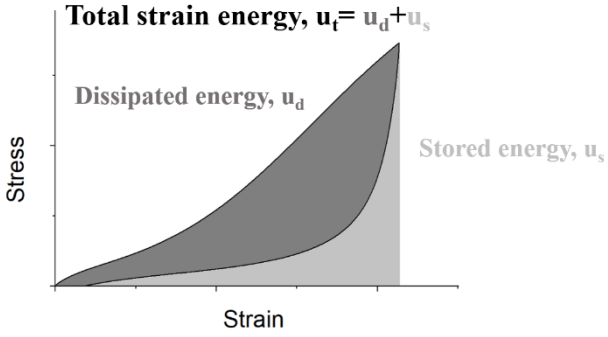


Figure 4. Total strain energy density and its components.

As it can be noticed in Figure 5, strain energy density, $u_t$, is higher for HNBR-PA than for HNBR, and this is due to a higher dissipated energy component, $u_d$. Otherwise, the two materials exhibit a similar stored energy component, $u_s$. In Figure 6, the two components have been represented as percentage of the overall strain energy density: HNBR-PA resulted to be a more dissipative material than HNBR and the range of deformations in which the dissipated energy is higher than the stored one is larger for this material than for HNBR.

#### 3.2.2 *Multi-cycle tests*

For HNBR, three consecutive cycles have been performed on each tested specimen. In Figure 7 there are the experimental curves of the multi-cycle loading-unloading tests. It can be seen that major softening is caused by the first loading: the loading curve of second and third cycles are comparable. Total strain energy and its stored and dissipated components have been calculated also for the second cycle, resulting similar to those of the third one.

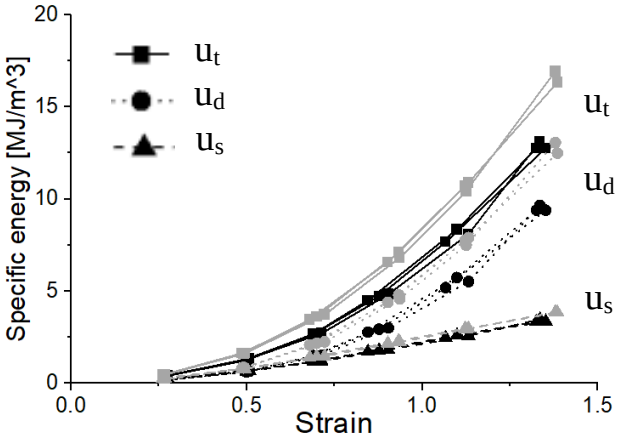


Figure 5. Strain energy densities in function of applied strain. In black HNBR, in grey HNBR-PA.

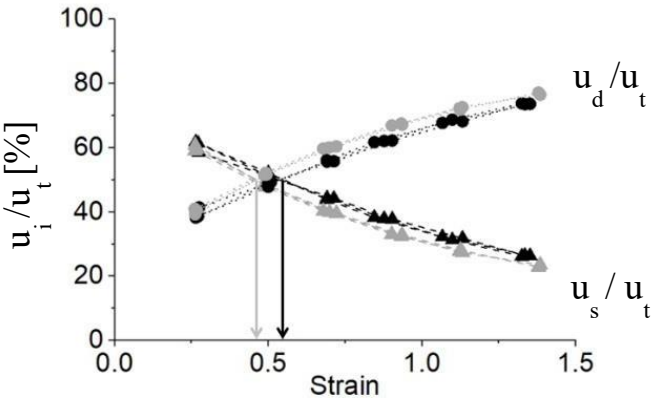


Figure 6. Dissipated and stored energy components as percentage of the total strain energy. In black HNBR, in grey HNBR-PA.

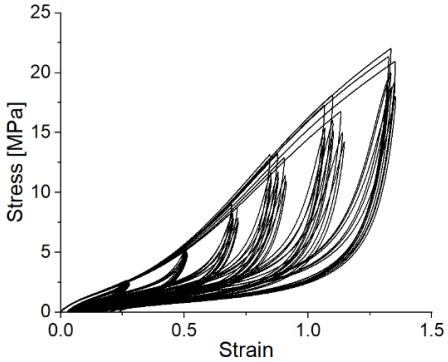


Figure 7. Multi-cycle loading-unloading tests of HNBR.

In Figure 8 total strain energy and its components have been represented for both virgin (first cycle, in black) and softened (second cycle, in grey) materials. The main observation is that total energy $u_t$ of the softened material is considerable smaller than that of the virgin material, due to a lower dissipated energy $u_d$, while elastic energies $u_s$ are comparable.

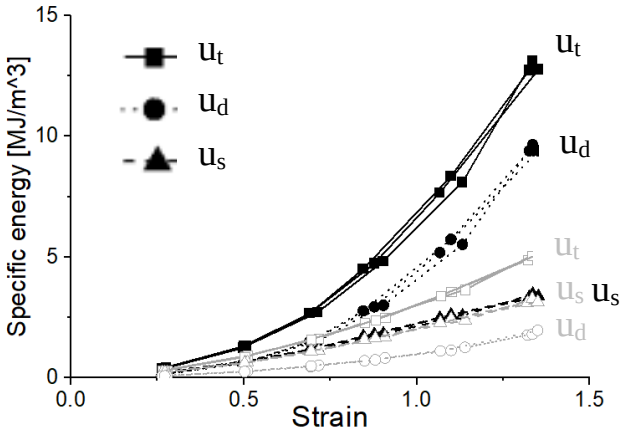


Figure 8. Strain energy densities as a function of the applied strain. In black virgin HNBR, in grey softened HNBR.

### 3.3 *Thermal treatment effect on the tensile behavior of strain-softened materials*

Two thermal treatments have been applied on softened materials with the aim of studying the thermally induced softening recovery: 24 h at 100°C or at 150°C. Preliminary tests on virgin materials have been performed in order to firstly evaluate if these thermal treatments may have any effect, such as a continuation of curing progress. As it can be noticed in Figure 9 and 10, both thermal treatments cause just a little increase in material stiffness, so their effect on curing can be considered not significant.

Single cycle loading-unloading tests have been carried out in uniaxial tensile loading conditions on specimens of HNBR and HNBR-PA up to a strain of about 1 and the softened materials have been thermally treated for 24 h at 100°C or at 150°C. In Figure 11, HNBR-PA loading curves are shown for virgin material (solid lines) and for specimens that have been treated after softening at 100°C (dotted lines) and at 150°C (dashed lines). It can be seen that, after a thermal treatment at 100°C, material recovers only at low strains while, after the treatment at 150°, the response of the material is comparable to that of the virgin one up to a strain of about 0.38 and is very close to it for larger strains. Similar results were obtained for HNBR, as shown in Figure 12.

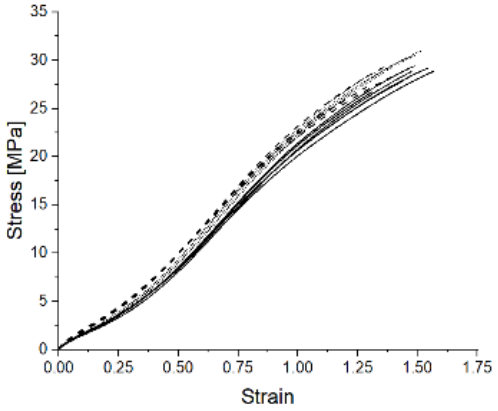


Figure 9. Stress-strain curves of HNBR-PA virgin material, before (solid lines) and after a thermal treatment of 24h at 100°C (dotted lines) or at 150°C (dashed lines).

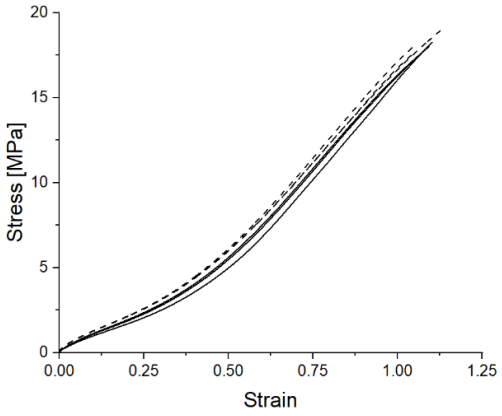


Figure 10. Stress-strain curves of HNBR virgin material, before (solid lines) and after a thermal treatment of 24h at 150°C (dashed lines).

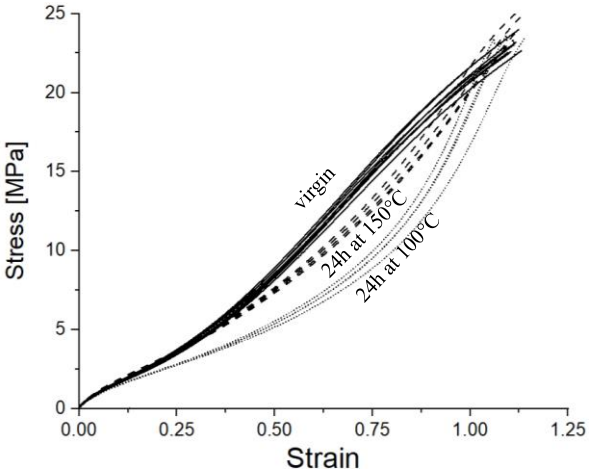


Figure 11. HNBR-PA loading curves of virgin material (solid lines) and of softened specimens kept for 24h at 100°C (dotted lines) and at 150°C (dashed lines).

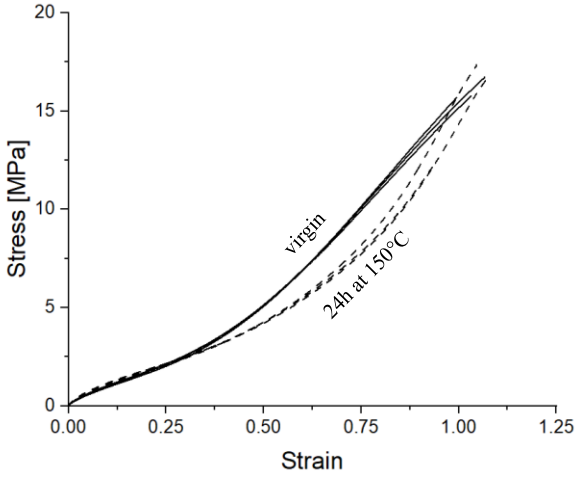


Figure 12. HNBR loading curves of virgin material (solid lines) and of softened specimens kept for 24h at 150°C (dashed lines).

### 3.4 *Fracture tests*

#### 3.4.1 *Pure shear*

Material fracture behaviour has been studied by performing fracture tests on notched specimens in pure shear loading conditions at the displacement rate of 75 mm/min. Fracture mechanics approach based on the J-integral (Rice 1968, Kim et al. 1989) has been adopted to calculate fracture toughness as

$$J_c = \eta \frac{U_t}{t(w - a_0)}$$

where $\eta$ is a dimensionless factor that depends on specimen geometry (equal to 1 for pure shear loading conditions), $U_t$ is the total input energy at crack onset calculated as the area under the force-displacement curve up to the fracture onset, t the specimen thickness, w the specimen width and $a_0$ the initial notch length.

In Figure 13 the values of J-integral at crack onset for the two materials are reported: the histogram shows that HNBR-PA exhibits a slightly higher fracture toughness. Figure 14 reports the values of the strains measured at crack onset on the initial notch plane, plotted versus the distance from the notch tip. In Figure 15 the values of the deformation close to the crack tip (at a distance of 0.37 mm), $\varepsilon_c$, and of the strain on the initial notch plane far from the crack tip, $\varepsilon_f$, are also reported. It can be seen that both the materials exhibit comparable strain values at fracture onset. Thus, the higher fracture toughness of HNBR-PA could be related to a higher strain induced energy dissipation in the material.

To evaluate the effect of a strain induced softening on material fracture toughness, softening should be carried out by straining up to deformations larger than the ones measured at fracture onset ($\varepsilon >> \varepsilon_c$). Experimental difficulties were encountered when strain induced softening was attempted by drawing the un-notched PS specimens: they always broke close to the clamping system at strain close to $\varepsilon_c$. Fracture tests where thus also performed on SENT specimens, after verifying no premature rupture of the un-notched tensile test pieces occurred during the loading-unloading cycles carried out to soften the material at strains larger than $\varepsilon_c$.

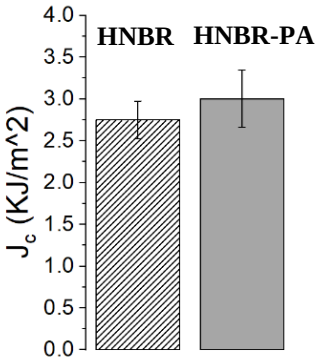


Figure 13. J-integral at crack onset for the studied materials.

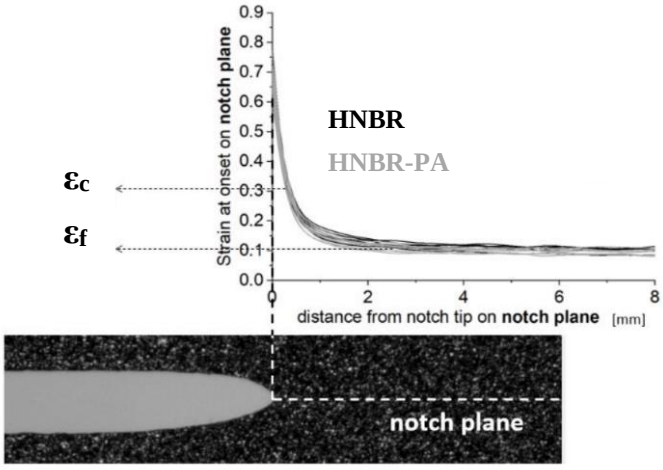


Figure 14. Deformations measured in the loading direction along the notch plane at crack onset for HNBR in black and HNBR-PA in grey.

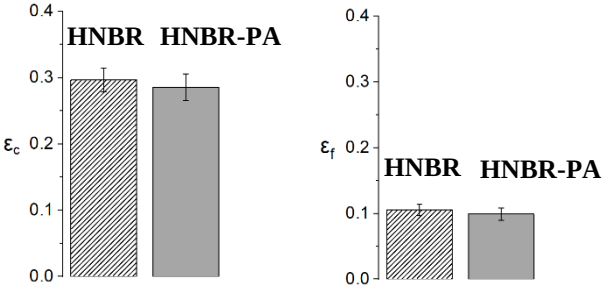


Figure 15. Strains values measured for the two materials at crack onset close to the crack tip and far from the crack tip.

### 3.4.2 *SENT*

Fracture tests on SENT specimens were carried out only on HNBR. Tearing energy formulation (Rivlin and Thomas 1953) has been used to calculate the fracture toughness (T)

$$T = k(\lambda_c) \frac{U_t}{t\, w\, h} a_0$$

with $k(\lambda) = \frac{2\pi}{\sqrt{\lambda}}$ (Greensmith 1963), where h is the gauge length and k a geometric factor dependent on $\lambda_c$, which is the draw ratio measured at crack onset far from the notch.

Tests have been carried out at the displacement rate of 10 mm/min both on virgin and softened material (preliminarily strained up to a deformation of about 1.1). The fracture behavior of the softened material has been studied also after performing a thermal treatment of 24h at 150°C. As reported in 3.3, this treatment allows an almost complete recovery of the deformation-induced softening in a strain range lower than 0.38, that is higher than $\varepsilon_c$ measured at fracture onset. In Figure 16, the tearing energy T calculated from fracture tests on virgin, softened and thermally treated softened material is reported. It can be observed that virgin material has a higher fracture toughness compared to the softened material. Moreover, it can be observed that after the thermal treatment the tearing energy results to be comparable to that of

the virgin material, suggesting a thermally induced softening recovery.

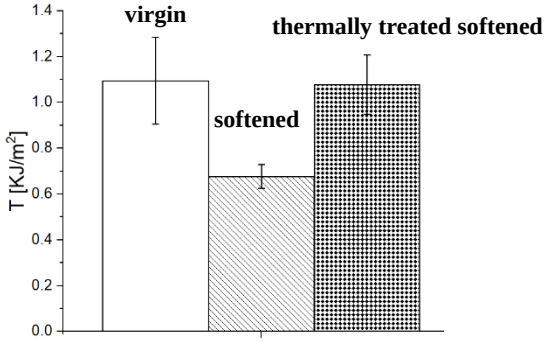


Figure 16. Tearing energy of virgin, softened and thermally treated softened HNBR.

## 4 CONCLUSIONS

After a preliminary analysis of the studied materials, a comparison of their fracture behaviour is reported. By performing fracture tests in pure shear loading conditions, it has been observed that, despite the deformation at crack onset reached by the two materials is comparable, HNBR-PA exhibits a slightly higher fracture toughness. This can be correlated to the fact that the dissipated strain energy density of HNBR-PA is larger than that of HNBR, in the whole strain range explored.

Moreover, it has been verified that, if a thermal treatment is applied after a preliminary strain induced softening, a recovery of this softening is possible. In particular, the higher the temperature of the treatment the larger the strain range in which the material behave like the virgin one.

In the last part, after the selection of a proper thermal treatment, fracture tests on virgin, softened and thermally treated softened HNBR have been performed, by carrying out tests on SENT specimens. The results show that softened material has a lower fracture toughness compared to the virgin material, while the thermally treated softened exhibits a toughness comparable to that of the virgin one, due to a material structure recovery.

## 5 REFERENCES


Agnelli, S.; Balasooriya, W.; Bignotti, F.; Schrittesser, B. On the experimental measurement of fracture toughness in SENT rubber specimens, Polymer Testing 87 (2020) 106508.

Blanchard, A. F.; Parkinson, D. Breakage of Carbon-Rubber Networks by Applied Stress. Ind. Eng. Chem. 1952, 44 (4), 799–812.

Bueche, F. Molecular Basis for the Mullins Effect. Journal of Applied Polymer Science 1960, 4 (10), 107–114.

Dannenberg, E. M.; Brennan, J. J. Strain Energy as a Criterion for Stress Softening in Carbon-Black-Filled Vulcanizates. Rubber Chemistry and Technology 1966, 39 (3), 597–608.

Diani, J.; Fayolle, B.; Gilormini, P. A Review on the Mullins Effect. European Polymer Journal 2009, 45 (3), 601–612.

Greensmith, H.W. (1963), Rupture of rubber. X. The change in stored energy on making a small cut in a test piece held in simple extension. J. Appl. Polym. Sci., 7: 993-1002.

Handbook of Synthetic Rubber, ARLANXEO (2021), p302-304.

Hanson, D. E.; Hawley, M.; Houlton, R.; Chitanvis, K.; Rae, P.; Orler, E. B.; Wrobleski, D. A. Stress Softening Experiments in Silica-Filled Polydimethylsiloxane Provide Insight into a Mechanism for the Mullins Effect. Polymer 2005, 46 (24), 10989–10995.

Harwood, J. A. C.; Payne, A. R. Stress Softening in Natural Rubber Vulcanizates. Part IV. Unfilled Vulcanizates. Journal of Applied Polymer Science 1966, 10 (8), 1203–1211.

Hemstede-van Urk, M.; Spanos, P.; Dodevski, J.; Kaiser, A.; Lieber, S.: Rubber World April: Therban HT: Polyamide reinforced HNBR with improved high temperature properties, (2020).

Houwink, R. Slipping of Molecules during the Deformation of Reinforced Rubber. 1956.

Kim, B. H.; Joe, C. R. Single Specimen Test Method for Determining Fracture Energy (Jc) of Highly Deformable Materials. Engineering Fracture Mechanics 1989, 32 (1), 155–161.

Kraus, G.; Childers, C. W.; Rollmann, K. W. Stress Softening in Carbon Black-Reinforced Vulcanizates. Strain Rate and Temperature Effects. Journal of Applied Polymer Science 1966, 10 (2), 229–244.

Laraba-Abbes, F.; Ienny, P.; Piques, R. A New 'Tailor-Made' Methodology for the Mechanical Behaviour Analysis of Rubber-like Materials: II. Application to the Hyperelastic Behaviour Characterization of a Carbon-Black Filled Natural Rubber Vulcanizate. Polymer 2003, 44 (3), 821–840.

Mullins, L. Effect of stretching on the properties of rubber. J Rubber Res 1948; 16:275–82.

Mullins, L. Softening of Rubber by Deformation. Rubber Chemistry and Technology 1969, 42 (1), 339–362.

Papkov, V. S.; Godovskii, Yu. K.; Bulkin, A. F.; Zhdanov, A. A.; Slonimskii, G. L.; Andrianov, K. A. Energy Investigation of the Softening of Siloxane Rubbers during Deformation. Polymer Mechanics 1975, 11 (3), 329–333.

Plagge, J.; Klueppel, M. Mullins Effect Revisited: Relaxation, Recovery and High-Strain Damage. Materials Today Communications, Volume 20, 2019, 100588, ISSN 2352-4928.

Rice, J. A Path Integral and the Approximate Analysis of Strain Concentration by Notches and Cracks. Journal of Applied Mechanics 1968, 35, 379–386.

Rigbi, Z. Reinforcement by Carbon Black Considered as a Rate Process. Kolloid-Z.u.Z.Polymere 1968, 223 (2), 127–134.

Rivlin, R.S. & Thomas, A.G. (1953), Rupture of rubber. I. Characteristic energy for tearing. J. Polym. Sci., 10: 291-318.

Yeoh, O.H. (2001) Analysis of deformation and fracture of 'pure shear' rubber testpiece, Plastics, Rubber and Composites, 30:8, 389-397.


## 6 ACKNOWLEDGMENTS


The research work was performed within the COMET-project "Polymers4Hydrogen" (project-no.: 21647053) at the Politecnico di Milano within the framework of the COMET-program of the Federal Ministry for Climate, Action, Environment, Energy, Mobility, Innovation and Technology and the Federal Ministry for Digital and Economic Affairs with contributions by Polymer Competence Center Leoben GmbH (PCCL, Austria), Montanuniversität Leoben (Department Polymer Engineering and Science, Chair of Chemistry of Polymeric Materials, Chair of Materials Science and Testing of Polymers), Technical University of Munich, Tampere University of Technology, Bundesanstalt für Materialforschung und -prüfung (BAM) and Arlanxeo Deutschland GmbH, ContiTech Rubber Industrial Kft., Peak Technology GmbH, SKF Sealing Solutions Austria GmbH, and Faurecia.